ChemComm

COMMUNICATION

A chiral spin crossover metal–organic framework†

Wei Liu,[a] Xin Bao,[b] Ling-Ling Mao,[a] Jiri Tucek,[c] Radek Zboril,[c] Jun-Liang Liu,[a] Fu-Sheng Guo,[a] Zhao-Ping Ni[a] and Ming-Liang Tong*[a]

Cite this: *Chem. Commun.*, 2014, 50, 4059

Received 22nd November 2013, Accepted 21st February 2014

DOI: 10.1039/c3cc48935c

www.rsc.org/chemcomm

A chiral metal–organic framework exhibiting spin crossover (SCO) property, $[Fe^{II}(mptpy)_2]\cdot EtOH\cdot 0.2DMF$ (1·solv), has been solvothermally synthesized through spontaneous resolution. It displays remarkable stability and two-step SCO at (T_{c1} = 200 K) and above (T_{c2} = 357 K) room temperature.

As a consequence of the splitting of the energy of the d orbitals into t_{2g} and e_g sets in an octahedral field, metal ions with configurations d^4 to d^7, particularly the Fe^{II} ion, can undergo SCO if appropriate ligand field strength is afforded. The switching between the high-spin (HS) and low-spin (LS) states may be driven by external stimuli such as temperature, pressure, light and magnetic field, resulting in alterable chemical and physical properties and thus leading to potential applications of SCO materials as molecular switches, molecular sensors, data storage and display devices.[1,2] Furthermore, developing SCO materials exhibiting multi-step spin transition around room temperature, which enables a larger information storage capacity, would be of great interest for their applications.

Particularly, the synthesis of new multi-functional materials is one of the most important trends in the SCO field, in which the SCO properties may be combined with other physical or chemical properties, such as magnetic coupling, liquid crystalline properties, non-linear optical properties and electrical conductivity.[3] In order to obtain novel magneto-optical materials, integrating chirality into SCO complexes would be a promising strategy. With conventional achiral optical recording media based on photochromic SCO compounds, the already stored data can be erased when the compounds are exposed to the light used to read the data by UV/Vis spectroscopy (destructive readout). The chiral SCO materials can exhibit nondestructive readout properties as revealed by optical rotation measurements.[4a] Although several combinations of the SCO cation with the anionic chiral magnetic framework,[4] chiral mononuclear SCO complexes[5] and a cyanide-bridged [CoFe] chain[3b] have been investigated, 2D or 3D SCO frameworks exhibiting inherent chirality are quite rare until now. A recent breakthrough was achieved by Ohkoshi *et al.* in a 3D chiral structured iron-octacyanoniobate where photomagnetism and chiral structure are coupled.[3c]

With the aim of exploring a multi-dimensional SCO system with chirality and higher critical temperature, we elaborately chose 3-methyl-2-(5-(4-(pyridin-4-yl)phenyl)-4*H*-1,2,4-triazol-3-yl)-pyridine (Hmptpy) as the ligand to coordinate with a Fe^{II} ion. Hmptpy can be viewed as a lengthened analogue of 3-(2-pyridyl)-5-(4-pyridyl)-1,2,4-triazolate which was previously demonstrated to be an appropriate ligand to construct highly stable SCO-MOFs.[6] It is expected that an additional benzene ring could enhance intermolecular interaction without disturbing ligand field strength and coordination behaviour a lot. Moreover, this kind of asymmetric ligand has rich coordination modes, in particular, chiral ones (Scheme S1, ESI†) that may result in optically active SCO materials, which make it more fascinating.

Crystals of **1**·solv (Fig. 1) were synthesized by reacting Hmptpy and $FeCl_2\cdot 4H_2O$ in a mixture of EtOH and DMF at 160 °C. Single crystals of **1**·solv crystallize in the chiral space group (either $P3_112$, **1**-P or $P3_212$, **1**-M) through spontaneous resolution, while the bulk sample is a racemic mixture. Each asymmetric unit contains half of the formula and the coordination environments of the Fe atoms have either *Δ* (**1**-P) or *Λ* (**1**-M) form (inset of Fig. 2a). Each Fe^{II} ion is *cis* coordinated to six N atoms from four μ-mptpy ligands and is further connected to four other Fe^{II} ions, thus forming a 4-connected 3D network. Topologically, every Fe^{II} ion can be seen as a four-connected node and every mptpy ligand acts as a linker. The 3D framework

[a] *School of Chemistry & Chemical Engineering, Sun Yat-Sen University, 510275 Guangzhou, P. R. China. E-mail: tongml@mail.sysu.edu.cn*
[b] *Department of Chemistry, School of Chemical Engineering, Nanjing University of Science and Technology, 210094 Nanjing, P. R. China*
[c] *Regional Centre of Advanced Technologies and Materials, Department of Experimental Physics, Faculty of Science, Palacky University, Slechtitelu 11, 783 71 Olomouc, Czech Republic*

† Electronic supplementary information (ESI) available: Synthesis, crystallographic information, TG-MS analysis, DSC, XRD patterns, variable temperature Raman spectra, and additional figures. CCDC 972750–972753. For ESI and crystallographic data in CIF or other electronic format see DOI: 10.1039/c3cc48935c

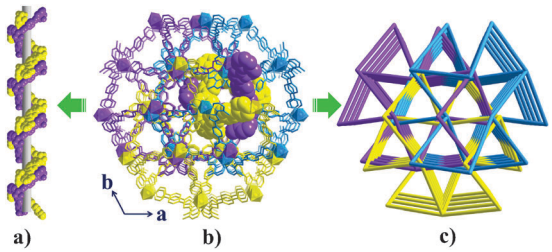

Fig. 1 (a) The 3_1 helical chains (**1**-P) viewed from the *a*-axis. (b) The 3-fold interpenetrated structure of **1**-P with a hexagonal helical channel along the *c*-axis highlighted (H atoms and guests are omitted for clarity). (c) The 3D framework of **1**-P possessing the **qtz** net topology.

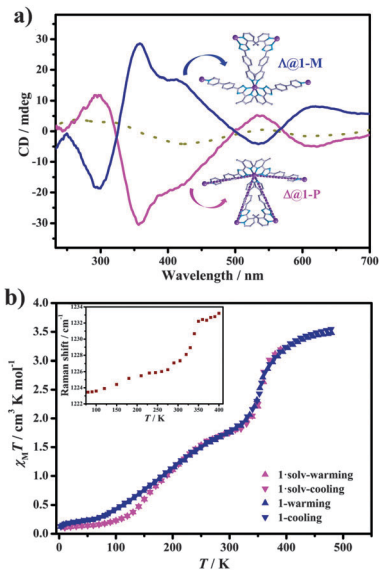

Fig. 2 (a) Bulk samples and single-crystal CD spectra. **1**-M (navy), **1**-P (magenta) and bulk samples (dark yellow); inset: ball and stick drawing of the coordination environments of the Fe atoms and the Hmptpy ligand in **1**·solv (H atoms are omitted for clarity). Color code: Fe^{II}, pink; N, blue; C, grey. (b) $\chi_M T$ *vs.* *T* for **1**·solv and **1**; inset: blue shift at 1222 cm^{-1} *vs.* *T* obtained from variable Raman spectra.

is characteristic of quartz (**qtz**) net topology with an Fe point symbol of $6^4.8^2$.[7] In contrast to the silica prototype, **1**·solv also contains a 3-fold screw axis in the *c* direction and the Fe^{II} ions running along this axis produce a right-handed helix in **1**-P (or a left-handed helix in **1**-M). The six helices are put together by sharing Fe^{II} ions. A consequence of lengthening the Si–O–Si connections by the replacement with Fe–mptpy–Fe is that there is room for the interpenetration of three identical but independent nets. The three nets are related to each other by rotation along the threefold *c* axis of 120° and they all have the same handedness. In spite of the interpenetration there are still voids along the *c* axis that accommodate disordered guests. These guests cannot be refined well in our crystallographic analysis, but can be determined by thermogravimetric-mass spectroscopy and elemental analysis as 1 EtOH and 0.2 DMF (Fig. S1, ESI†).

The occurrence of SCO was detected by comparing structural features of **1**-P as a representative at 150 K, 293 K and 373 K (Table S1, ESI†). The effective indicators, octahedral distortion parameter Σ and variation of $Fe–N_{average}$ are listed in Table S2 (ESI†). The $Fe–N_{average}$ bond length of 2.021 Å at 150 K indicates that most Fe^{II} ions are in the LS state. Upon warming to 293 K, the bond length increases to 2.077 Å. While at 373 K, the value showed a sizable increase to 2.165 Å, indicating that most Fe^{II} ions are in the HS state.

In order to confirm the supramolecular enantiomeric nature of **1**·solv, both individual crystals and bulk samples were characterized by solid-state circular dichroism (CD) spectroscopy in KCl pellets (Fig. 2a and Fig. S2, ESI†). The signal of bulk samples is hardly recognized, while obvious cotton effects are observed for individual crystals, showing two positive peaks at 299 nm and 536 nm, as well as three negative peaks at 355 nm, 405 nm and 610 m for **1**-P. Opposite signals at the same wavelengths for **1**-M are observed too, indicating the spontaneous resolution process. As for the framework's stability, TG analysis shows no occurrence of decomposition until 735 K except weight loss of guests (6.7%) centred at 432 K while the variable temperature powder X-ray diffraction patterns (Fig. S3, ESI†) reveal that the framework remains unaltered at least up to 653 K, which is the upper limit of experimental conditions.

The magnetic susceptibilities of both the as-synthesized sample **1**·solv and the desolvated sample **1** were measured in an applied field of 2000 Oe. The results are shown in Fig. 2b in the form of $\chi_M T$ *versus* *T* plots, showing the occurrence of two-step SCO behaviour (T_{c1} = 200 K, T_{c2} = 357 K) without thermal hysteresis. The measurement for **1**·solv was carried out below 390 K in order to avoid the escape of solvent. The $\chi_M T$ value at 390 K is 3.19 emu mol^{-1} K, indicating that most Fe^{II} ions are in the HS state. Upon cooling, the $\chi_M T$ value continuously decreases and then reaches a pseudo-plateau between 310 K and 270 K, with a value of about 1.75 emu mol^{-1} K, which is expected for an approximately 50% distribution of the HS and LS states (intermediate state, IP). With further decrease of the temperature, the $\chi_M T$ value decreases to a minimum value below 80 K of approximately 0.2 emu mol^{-1} K, implying the completion of SCO. Such behaviour is consistent with the variable-temperature Raman spectra in which the peak at 1223 cm^{-1} exhibits a blue shift to 1233 cm^{-1} upon heating rather than the ordinary red shift due to the lattice expansion (inset of Fig. 2b and Fig. S5, ESI†). The desolvated sample, **1**, shows a highly similar SCO behaviour to **1**·solv with the $\chi_M T$ value reaching 3.54 emu mol^{-1} K at 480 K, demonstrating that almost all Fe^{II} ions are in the HS state.

The two-step SCO nature of this 3D framework presents a new case with crystallographically equivalent metal centers that undergo stepped SCO.[8] One possibility for this phenomenon is an overall structural rearrangement such as symmetry breaking in the IP phase (long range order).[8d] But no crystallographic evidence for such an event was observed. While the evidence for symmetry breaking can be very subtle that it is not always detectable using a standard laboratory X-ray diffraction setup, thus, this type of transition cannot be eliminated here. The other possibility is the random arrangement of HS and LS irons in IP states.[8e] A variable temperature Raman experiment was

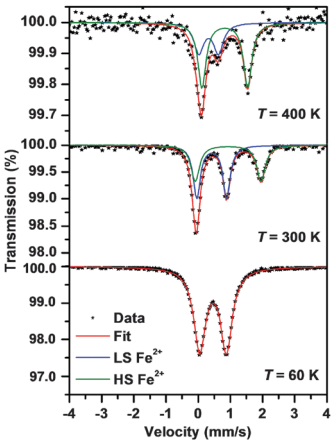

Fig. 3 Mössbauer spectra of **1**·solv at 60 K, 300 K, and 400 K.

undertaken to obtain some information.[9] Apparent discontinuities are observed from 80 K to 390 K (Fig. S5, ESI†), indicating the possibility of synergetic structural rearrangement of the whole lattice.

In differential scanning calorimetry (DSC) measurements, the sample of **1**·solv was first heated from 300 K to 720 K (Fig. S4, ESI†). It gives two peaks centred at 358 K and 445 K (ΔH_1 = 10.5 kJ mol^{-1}, ΔS_1 = 29.1 J K^{-1} mol^{-1}; ΔH_2 = 37.6 kJ mol^{-1}, ΔS_2 = 84.5 J K^{-1} mol^{-1}), corresponding to the second step transition and the loss of guest molecules, respectively. The subsequent measurement upon cooling and the second cycle of heating and cooling represent only the spin transition for **1**.

In order to get a deeper insight into the spin state and the corresponding transition process, the ^{57}Fe Mössbauer spectra of **1**·solv were recorded at 60 K, 300 K, and 400 K (Fig. 3 and Table S3, ESI†). At 60 K, the spectrum can be fitted with one doublet (δ = 0.46 and ΔE_Q = 0.83 mm s^{-1}, where δ is the isomer shift and ΔE_Q the quadrupole splitting), the hyperfine parameter values of which are characteristic of a single LS Fe^{II} site. Upon warming, the 300 K Mössbauer spectrum (*i.e.*, at a temperature in the plateau) shows the emergence of an additional doublet corresponding to HS Fe^{II} sites, implying that about half (45%) of the iron centres have undergone the LS → HS transition (LS Fe^{II}: δ = 0.42, ΔE_Q = 0.93 mm s^{-1}; HS Fe^{II}: δ = 0.93, ΔE_Q = 2.04 mm s^{-1}). Upon warming to 400 K, most Fe^{II} sites accomplish spin transition, however, some LS Fe^{II} sites were still observed (LS Fe^{II}: δ = 0.33, ΔE_Q = 0.61 mm s^{-1}; HS Fe^{II}: δ = 0.83, ΔE_Q = 1.42 mm s^{-1}), which agrees with the magnetic susceptibility data.

In summary, we have demonstrated a very rare example of chiral 3D SCO-active MOF materials. The structure has a triply interpenetrated coordination network with quartz-like chiral topology. Magnetic study shows that it exhibits two-step spin transition behaviour with a plateau spanning room temperature. Such SCO behaviour is further confirmed by Raman spectroscopy, DSC analysis and ^{57}Fe Mössbauer spectroscopy.

This work was supported by the "973 Project" (2012CB821704 and 2014CB845602), Program for Changjiang Scholars and Innovative Research Team in University of China (IRT1298), and the NSFC (Grant no. 91122032, 21371183, 21201182 and 21121061). The authors acknowledge the support from the Operational Program Research and Development for Innovations – European Regional Development Fund (CZ.1.05/2.1.00/03.0058) and the Operational Program Education for Competitiveness – European Social Fund (CZ.1.07/2.3.00/20.0058) of the Ministry of Education, Youth and Sports of the Czech Republic.

Notes and references

1 (*a*) M. A. Halcrow, *Spin-crossover Materials: Properties and Applications*, John Wiley & Sons, 2013; (*b*) M. A. Halcrow, *Chem. Soc. Rev.*, 2011, **40**, 4119.
2 (*a*) J.-F. Létard, P. Guionneau and L. Goux-Capes, *Spin Crossover in Transition Metal Compounds III*, Springer, 2004, pp. 221–249; (*b*) A. Bousseksou, G. Molnár, L. Salmon and W. Nicolazzi, *Chem. Soc. Rev.*, 2011, **40**, 3313; (*c*) O. Kahn and C. J. Martinez, *Science*, 1998, **279**, 44; (*d*) I. Šalitroš, N. Madhu, R. Boča, J. Pavlik and M. Ruben, *Monatsh. Chem.*, 2009, **140**, 695.
3 (*a*) S. Hayami, K. Danjobara, K. Inoue, Y. Ogawa, N. Matsumoto and Y. Maeda, *Adv. Mater.*, 2004, **16**, 869; (*b*) N. Hoshino, F. Iijima, G. N. Newton, N. Yoshida, T. Shiga, H. Nojiri, A. Nakao, R. Kumai, Y. Murakami and H. Oshio, *Nat. Chem.*, 2012, **4**, 921; (*c*) S.-i. Ohkoshi, S. Takano, K. Imoto, M. Yoshikiyo, A. Namai and H. Tokoro, *Nat. Photonics*, 2014, **8**, 65.
4 (*a*) Y. Sunatsuki, Y. Ikuta, N. Matsumoto, H. Ohta, M. Kojima, S. Iijima, S. Hayami, Y. Maeda, S. Kaizaki, F. Dahan and J. P. Tuchagues, *Angew. Chem., Int. Ed.*, 2003, **42**, 1614; (*b*) Y. Sunatsuki, R. Kawamoto, K. Fujita, H. Maruyama, T. Suzuki, H. Ishida, M. Kojima, S. Iijima and N. Matsumoto, *Coord. Chem. Rev.*, 2010, **254**, 1871.
5 M. Clemente-León, E. Coronado, C. Martí-Gastaldo and F. M. Romero, *Chem. Soc. Rev.*, 2011, **40**, 473.
6 (*a*) X. Bao, P. H. Guo, J. L. Liu, J. D. Leng and M. L. Tong, *Chem.–Eur. J.*, 2011, **17**, 2335; (*b*) X. Bao, P.-H. Guo, W. Liu, J. Tucek, W.-X. Zhang, J.-D. Leng, X.-M. Chen, I. y. Gural'skiy, L. Salmon and A. Bousseksou, *Chem. Sci.*, 2012, **3**, 1629.
7 B. F. Hoskins, R. Robson and N. V. Scarlett, *Angew. Chem., Int. Ed.*, 1995, **34**, 1203.
8 (*a*) D. Boinnard, A. Bousseksou, A. Dworkin, J. M. Savariault, F. Varret and J. P. Tuchagues, *Inorg. Chem.*, 1994, **33**, 271; (*b*) D. Chiruta, J. Linares, M. Dimian, Y. Alayli and Y. Garcia, *Eur. J. Inorg. Chem.*, 2013, 5086; (*c*) D. Chernyshov, M. Hostettler, K. W. Törnroos and H. B. Bürgi, *Angew. Chem., Int. Ed.*, 2003, **42**, 3825; (*d*) G. J. Halder, K. W. Chapman, S. M. Neville, B. Moubaraki, K. S. Murray, J.-F. Létard and C. J. Kepert, *J. Am. Chem. Soc.*, 2008, **130**, 17552; (*e*) C. M. Grunert, J. Schweifer, P. Weinberger, W. Linert, K. Mereiter, G. Hilscher, M. Müller, G. Wiesinger and P. J. van Koningsbruggen, *Inorg. Chem.*, 2004, **43**, 155.
9 T. Forestier, S. Mornet, N. Daro, T. Nishihara, S.-i. Mouri, K. Tanaka, O. Fouché, E. Freysz and J.-F. Létard, *Chem. Commun.*, 2008, 4327.